RSC Advances

This article can be cited before page numbers have been issued, to do this please use: N. KHEIRABADI, *RSC Adv.*, 2016, DOI: 10.1039/C5RA27922D.

ROYAL SOCIETY OF CHEMISTRY

www.rsc.org/advances

View Article Online
DOI: 10.1039/C5RA27922D

Li-doped graphene for spintronic applications

Narjes Kheirabadi [1,2]

[1] Department of Physics, Iran University of Science and Technology, Narmak, Tehran, Iran, 1684613114.

[2]Department of Physics, Lancaster University, Lancaster LA1 4YB, United Kingdom.

View Article Online
DOI: 10.1039/C5RA27922D

Abstract

Generating spintronic devices has been a goal for the nano science. Here, Li-doped graphene flakes has been suggested for spintronic applications. To aim this goal, density function theory has been used to determine magnetic phases of monolayer and bilayer doped graphene nanoflakes. Adsorption energies, spin polarizations, electronic gaps, magnetic properties and robustness of spin-polarized states have been studied in the presence of dopants and second layers. Based on these results, graphene flakes have been introduced as single molecular magnets and spin amplifiers for room temperature applications. It has been determined that for bilayer flakes with two layers of different sizes, molecular orbitals switch between the layers around the Fermi level. Based on this switch of molecular orbitals in a bilayer graphene flake, spin on/off switches and spintronic memory devices could be achievable.

View Article Online
DOI: 10.1039/C5RA27922D

Introduction

Parallel to the development of the technology, molectronic, molecular electronic, explore new applications for materials, where quantum mechanics dominates electron kinetic behaviour [1, 2]. One dominant intriguing aspect of molectronic is related to spintronic applications. For spintronic applications, single molecular magnets (SMMs), magnetic molecules with stable magnetization at room temperature, have a special role [3-7]. SMMs can be used as ferromagnetic materials (FM); magnets with antiparallel spin orientation between two edges. In addition, FMs are the basis of spintronic devices, i.e. spin amplifiers, and those devices which magnetically store information at a molecular level.

When a current passes through a SMM, the current will be spin polarized as do a spin amplifier. A SMM spin amplifier conducts a very high spinpolarized current whose magnetization is parallel to the SMM magnetization. The time interval in which a spinpolarized current passes across the molecule is equivalent to the relaxation time. This phenomenon is named giant spin amplification [8, 9]. In fact, for large currents, this process can lead to a selective drain of spins with one orientation from the source electrode, thus it transfers a large amount of magnetic moment from one lead to the another [4].

The high coherence time, the absence of conformational changes, weak spin-orbit and hyperfine interactions of carbon (C) atoms make the development of carbon based SMMs more desirable [4, 10]. Between all of carbon based structures, the hexagonal arrangement of carbon atoms in two dimension, graphene, is more intriguing. The low efficiency of the spin relaxation up to a nanosecond [11-13], the scalability of the total spin, and graphene stability up to room temperature make graphene based materials excellent candidates for spintronic devices [14-17]. Furthermore, it has been shown that magnetic graphene nanoflakes (GNFs) potential for an extremely long spin relaxation and decoherence time, with weak coupling between electron spins, and long-range magnetic order[18].

It is noteworthy that GNFs transport properties can be changed with the application of the electric [19] and magnetic fields [20], additional layers [21], and geometry [22-25]. Consequently, the ability to modify the electronic properties of finite-sized graphene materials by varying their size, shape, defects and edge orientation is an important part of molectronic research.

View Article Online
DOI: 10.1039/C5RA27922D

In laboratories, experiments indicate that spintronic devices based on the GNF are achievable by modern nano-scale fabrications. Some methods to isolate GNFs are nano cutting by electro-beam lithography [26, 27], C_{60} transformation [28], heat-induced fractionalization of graphite [29], heat-induced conversion of nanodiamonds [30, 31] and unzipping of carbon nanotube [32]. Moreover, bilayer graphene can be defined by top gates [33], and it can be produced asymmetrically by use of an epitaxial growth method [34]. In addition, there are some experiments have worked on GNFs electronic properties. Some of these experiments are charge detection in bilayer GNFs, observation of spin states in GNF [20, 35], and observation of excited states in quantum dots [36, 37].

From the theoretical part of view, it is determined that some doped graphene nanoribbons could be FM [38], where the edge effect is of great importance for spin related properties [39]. Indeed, graphene nanoribbins have a magnetic insulating ground state with FM ordering at each zigzag edge [40-42]. However, there are not many cases studied magnetic properties of doped graphene flakes, especially bilayer ones. Consequently, the study of these SMMs is a missing part of molectronic [43]. In addition, the preservation of intrinsic properties for non-destructive readout of the spin states is an open issue [43].

The aim of this theoretical study is to suggest room temperature magnets. While, the control of a unidirectional logic flow is important for spintronic applications, the molecular orbital view provides a better understanding of the intermolecular transport phenomena. It also connects the analysis of the wave function to the intuitive quantum interference effects [44]. In fact, current study determines a reasonable correlation between the quantum interference and orbital interaction pictures. Based on this type of study, some suggestion for spintronic devices have been proposed.

Systems Geometry and Computational Details

In this article, properties of monolayer (Fig.1) and bilayer (Fig.3), lithium (Li)-doped hexagonal shaped GNFs have been studied. Because of the predicted important role of alkali-metal decorated graphene [45] and specially Li [46, 47], we have used this element as a dopant. The Li-doped GNFs are also hydrogen(H) terminated, in order to remove the effect of dangling bonds. The size of monolayer and doped cases is related to the total number of C atoms in their structure. For bilayer flakes, the size of the flake is considered to be equal to the size of its larger layer.

View Article Online
DOI: 10.1039/C5RA27922D

In the present work, we use whole-electron broken symmetry and first principles density function theory (DFT) calculations. The basis is 6-31g*, and the hybrid exchange-correlation functional is Becke, three-parameter, Lee-Yang-Parr (B3LYP) [48, 49] employing the Gaussian 03 software package [50] to verify the existence of the magnetic phases. The goal is answering some key questions about doped graphene magnetic properties.

First, the robustness of the spin-polarized states in the presence of both impurities and the second layer will be studied. The answer to this question is scientifically interesting for better understanding of the physical mechanism of spin polarization in the hexagonal nanoflakes. It has also important technological implications in the reliability of a doped hexagonal nanoflake as a new class of SMM for spintronic applications [43].

View Article Online
DOI: 10.1039/C5RA27922D

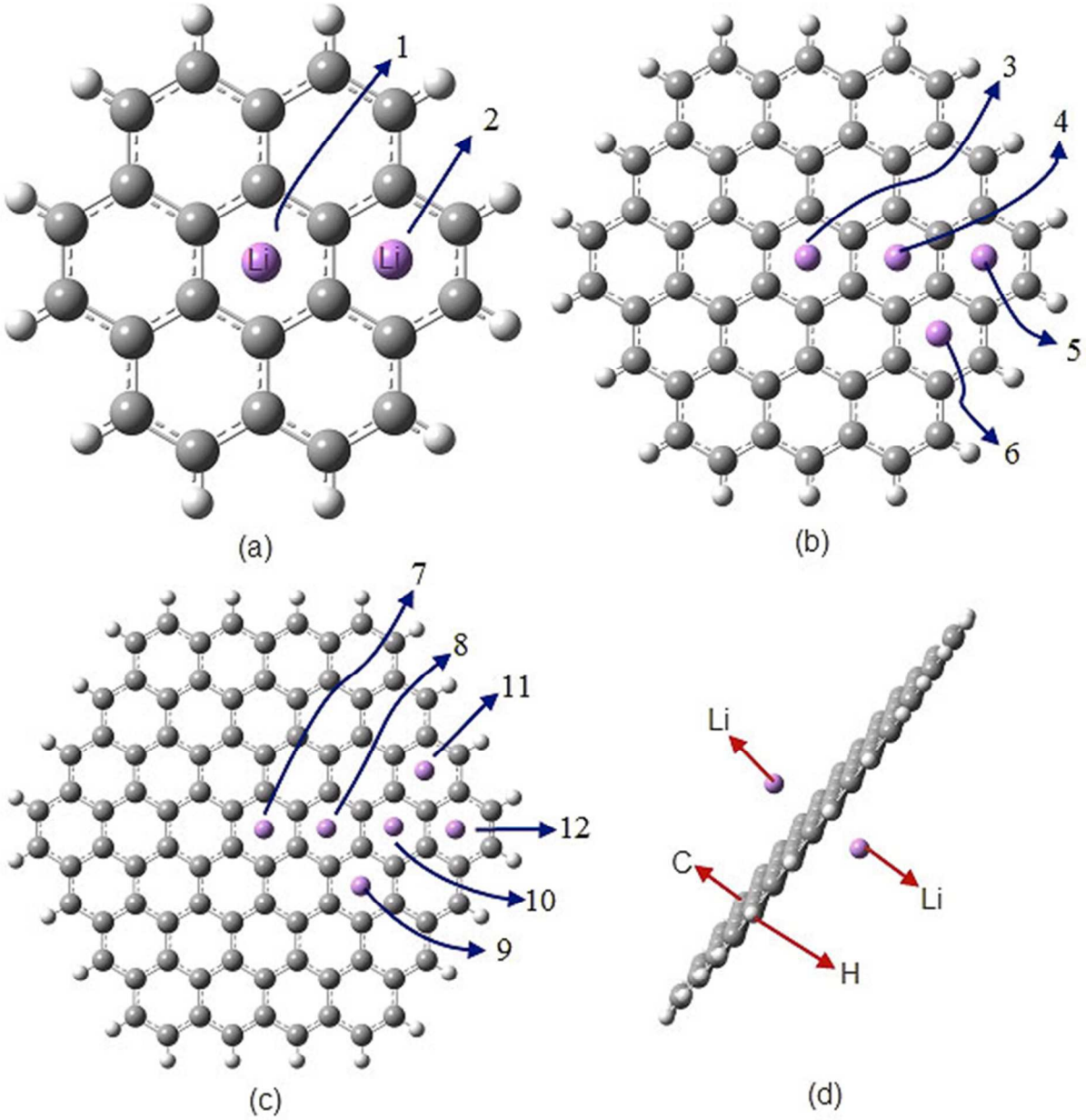

Fig. 1.Monolayer Li-doped GNFs. C, H and Li atoms are respectively grey, white and violent. (a) Two different $LiC_{24}H_{12}$ flakes (number 1 and 2). (b) Four distinct $LiC_{54}H_{18}$ flakes (number 3, 4, 5 and 6). (c) Six dissimilar Li $C_{92}H_{24}$flakes (flakes number 7 through 12). (d) $Li_2C_{92}H_{24}$, a flake number 13, doped by two Li atoms[51].

Second, the author will discuss how the magnetic structure of hexagonal nanoflakes changes with the size of the layer. In addition, the change of a doped GNF to have a magnetic ground state, and magnetic properties of bilayer flakes will be discussed. Furthermore, band gaps, and the magnetization of graphene flakes have been calculated as a function of second layer, and

View Article Online
DOI: 10.1039/C5RA27922D

adsorbed Li distance from the centre of the flake. In addition, to study the graphene magnetization and its applications, molecular orbital theory will be employed. Finally, based on results of this study, some suggestions for the C based spintronic amplifier, the spin on/off switch, and the spin based memory device will be determined.

Results

Monolayer GNFs

In this section, we have studied 13 distinctive Li-doped GNFs (Fig.1). The flakes have been arranged by the size and the distance of Li atoms from the centre of the flake. Consequently, flake NO.1 to NO.2, have the same size. Flakes NO.3 to NO.6 and flakes NO.7 to NO.13 are two other size groups. The result of calculations are illustrated in the Fig.2 and have been summarized in table.1.

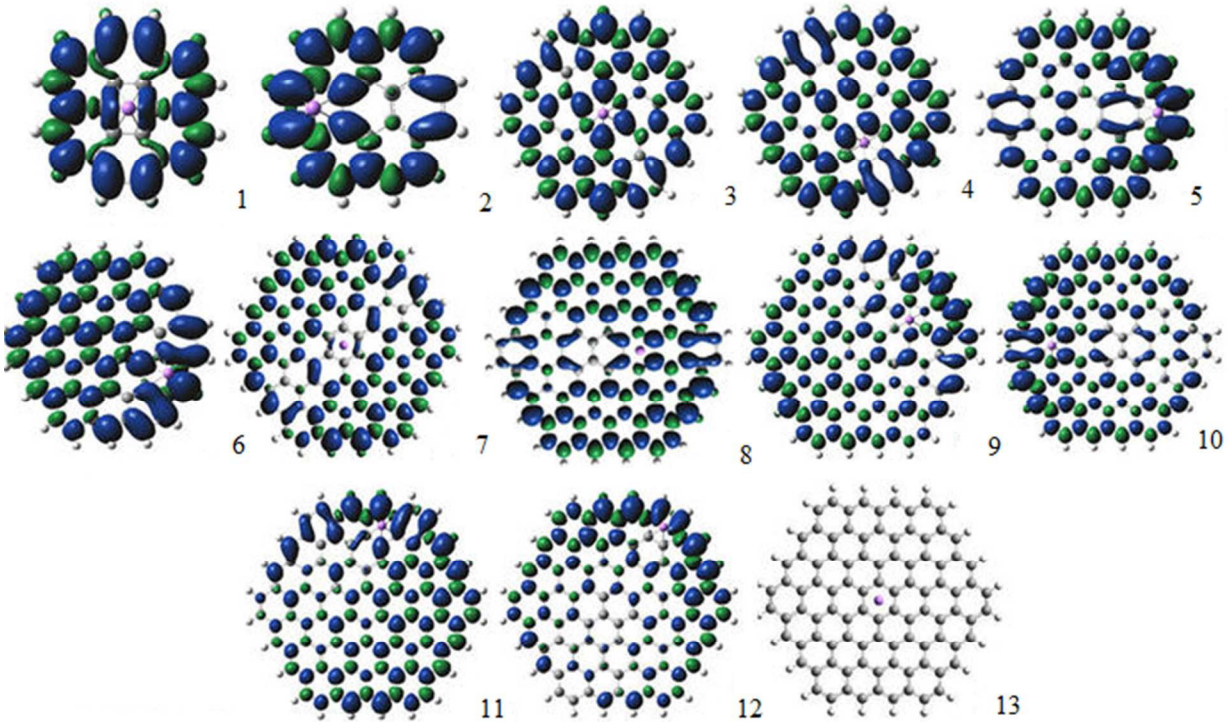

Fig.2. Studied monolayer Li-doped GNFs. The electron density from spin density is depicted in this figure. The isosurface value is±0.0004 electrons per cubic atomic unit for positive values in the blue and negative values in the green.

The relative stability and the highest occupied molecular orbital-lower unoccupied molecular orbital (HOMO-LUMO) gap of some of these flakes have been studied before [52]. However,

View Article Online
DOI: 10.1039/C5RA27922D

here, these properties have been studied for a larger group of Li-doped graphene. Flakes 5, 6, and 9 are newly considered flakes; the new results are consistent with results in Ref [52].

According to Ref.[52], edge states are generally more stable. This result has also been confirmed for a larger group of Li-doped GNFs. To describe it in detail, according to the table.1, adsorption energies of flakes NO.5 and NO.6, which have a Li atom nearer to the edges, arerespectively-0.024 and -0.0234 eV; more than flakes NO.3 (-0.017) and 4 (-0.017eV). In addition, for the flake NO.9, the adsorption energy (-0.025eV) is slightly red shifted relative to flakes NO.10 to NO.12 (-0.026, -0.032 and-0.032eV). However, the flake NO.9 has more adsorption energy relative to flakes NO.7 and 8 (-0.023 and-0.024eV) whose adsorbent is nearer to the edge.

The ultimate goal of graphene in the next generation electronic is to realize graphene based circuits [39, 53]. In fact, the same hexagonal carbon structures build excellent connections in a circuit. Consequently, graphene doped Li has an additional advantage. It is possible to build a unique circuit of both FM and NM phases by use of Li-doped graphene. The single electron of a Li atom breaks the symmetry between spin up and spin down states. As it is clear in Fig. 2, all doped graphene with one Li atom are FM [15], but a flake doped by two dopants is NM. This NM flake does not have any localized spin polarized states even at the edges.

For a better spin polarized current conduction, to join in a circuit, a contact group should be attached to localized orbitals [54]. From a qualitative analysis of the spin density maps in Fig.1, in flakes with Li adsorbed on the edge, where spin polarization is localized, the middle part has less spin polarized regions. When the Li atom is adsorbed on a symmetry line pass through two carbon rings with two H atoms, the distribution of spin up density is stronger than spin down density around that symmetry line (so that spin up states in the centre make a tunnel-like spin up zone).

As for the gap, all the flakes doped by one Li atom are spin polarized. The alpha gap is also red shifted by increasing of the flake size; as is the beta gap. According to Fig.1, the alpha gap for flakes NO.5, 6 and 9 are 1.02, 0.97, 0.68eV, correspondingly. Furthermore, the beta gaps are 2.67, 2.68 and 1.97eV, respectively. Consequently, our results confirm previous results about gap change according to the flake size and the distance from edge states [52].

Because of the different spin distribution population, each flake has distinctive FM properties. Here, the difference between the highest and the lowest spin polarization of C atoms has been selected as a factor to evaluate spin polarization of the flakes (table 1).

View Article Online
DOI: 10.1039/C5RA27922D

Table 1: Muliken spin density variation interval of monolayer GNFs. The difference between the highest and the lowest spin polarization of C atoms has been used to evaluate the spin polarization of flakes. Flake No.0 is a benzene ring doped by one Li atom in the centre.

Flake NO.	0	1	2	3	4	5	6	7	8	9	10	11	12
Polarization (Mulliken atomic spin densities)	0.12	0.28	0.27	0.25	0.26	0.30	0.30	0.20	0.33	0.26	0.24	0.25	0.33

According to table.1, those flakes with a Li atom nearer to boundary H atoms are better FM. For instance, the Li atom in flake NO.7 is adsorbed in the centre (Fig.2), far from edges; so, it has the least amount of the magnetization (table.1). These results show that the increase of the temperature which moves Li to the edge [55] is a factor which increases FM properties. Consequently, FM properties of suggested amplifiers could act well at room temperature.

The flake size is another important factor which affects magnetization. Between studied flakes, greater flakes have generally a stronger distribution of spin through the flake. The larger flakes, in which Li is adsorbed on a ring with two H atoms, are the best spin amplifiers. This note is a good reason to use a Li-doped graphene as a spin amplifier. Such structures are also more stable. For example, between flakes NO.2, 5 and 12 which have a Li atom at the edge, flake NO.2 whose C atoms are fewer is less spin polarized. In contrast, flake NO.12 with the largest size and the largest amount of spin polarization. Consequently, because of the graphene high spin life time and Li-doped graphene FM properties, considered bilayer flakes are room temperature SMMs.

SMM NO.12 is the best candidate for gigantic spin amplification and SMM applications. It is also predictable that the spin polarized current display a high spin polarization for a time equivalent to the relaxation time of graphene. Consequently, SMMs and similarly giant spin amplifications are achievable by use of suggested GNFs. The possibility of having a better spin amplifier based on even larger graphene flakes is also predictable.

Bilayer Graphene Flakes

To consider effects of an additional layer on magnetic properties of GNFs, a second layer has been added to monolayer flakes. Here, bilayer structures have been arranged according to the number of C atoms and the Li distance from the centre (Fig.3). According to Fig.3, we have studied bilayer flakes with both layers of unlike and equal size. Moreover, different positions for

View Article Online
DOI: 10.1039/C5RA27922D

an adsorbent Li atom and the second layer have been considered. Results for these flakes have been gathered in Fig.3 and table2. It is worthy to mention that, because DFT is based on whole electron calculations, the radius of the largest-considered monolayer GNF is larger than that of the studied bilayer GNFs.

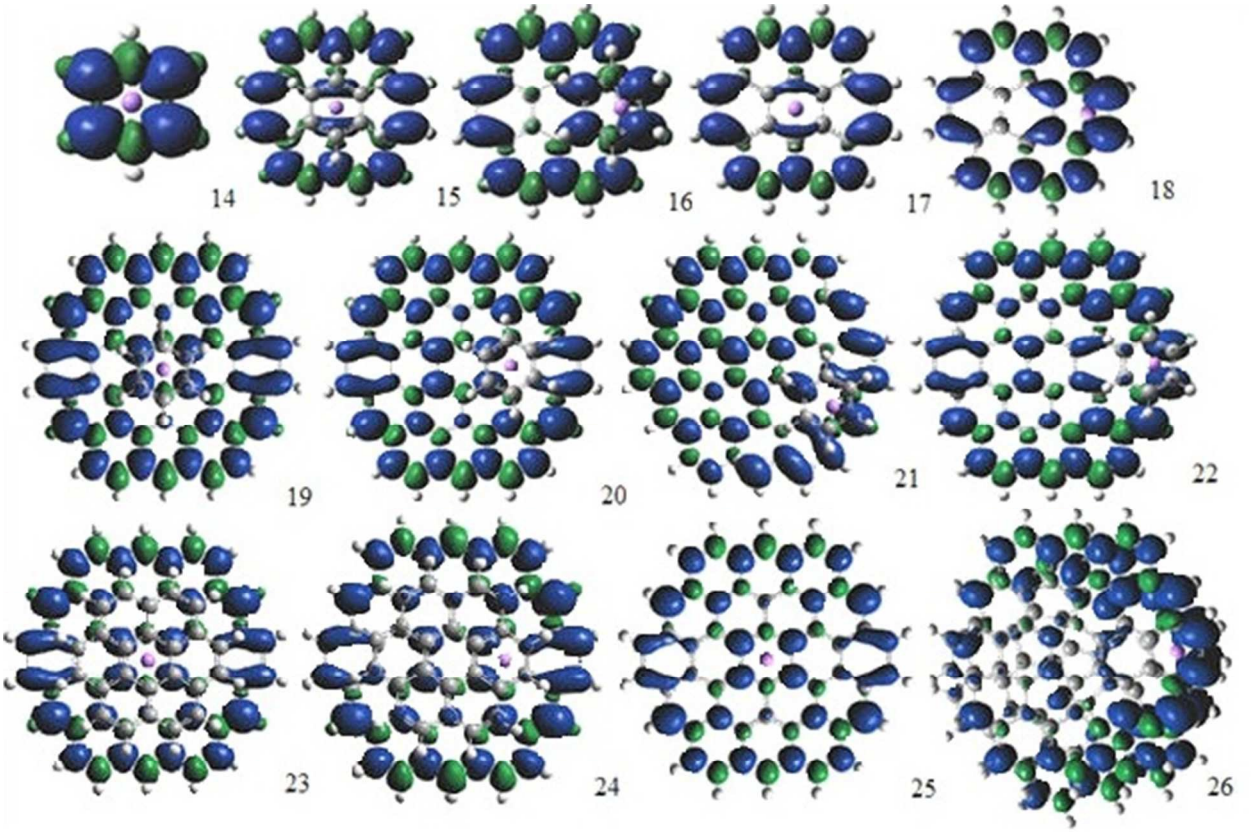

Fig.3.Studied bilayer GNFs. The isosurface value is ±0.0004 electrons per cubic atomic unit for positive values in the blue and negative values in the green.

View Article Online
DOI: 10.1039/C5RA27922D

Table2.Results of DFT calculations for bilayer GNFs. Here, the results for the adsorption energy, the spin polarization, and alpha and beta gaps of bilayer GNFs have been gathered.

NO.	Adsorption energy (eV)	Spin-polarization (Mulliken atomic spin densities)	Alpha/Beta gap (eV)
14	-0.027	0.22	1.32/5.86
15	-0.034	0.28	0.73/3.28
16	-0.039	0.23	1.1/3.67
17	-0.033	0.14	0.82/3.54
18	-0.043	0.13	0.87/3.57
19	-0.050	0.20	0.79/2.62
20	-0.049	0.24	0.82/2.62
21	1.444	0.29	0.91/2.67
22	-0.053	0.29	0.95/2.65
23	-0.043	0.20	0.64/2.49
24	-0.047	0.25	0.61/2.47
25	-0.046	0.10	0.61/2.51
26	-0.046	0.15	0.60/2.59

The arrangement of the flakes based on their stability is 21, 14, 17, 15, 16, 23, 18, 25, 26, 24, 20, 19 and 22. For relative stability, a particular rule has not been found. Unlike single layers, the total number of C atoms is not a determining factor for the amount of adsorption energy. For instance, flake NO.22 has fewer C atoms relative to flake NO.24 and NO.25, but its adsorption energy is red shifted. In contrast, flake NO.18, which has more C atoms relative to flakes NO.16

View Article Online
DOI: 10.1039/C5RA27922D

and NO.15, is more stable than both of those. However, between similar flakes, those which are doped by a Li atom and the second layer nearer to the edge are steadier.

According to table 2, between flakes 23 and 24, the latter whose Li atom is nearer to the edge is more stable; same about the flake NO.15 relative to 16, and NO.25 comparative to 26. Flake NO.22 is more stable than flake NO.20, and flake NO.20 adsorption energy is red shifted relative to the flake No.19. It is the same for the flake NO.16 relative to the flake NO.15. It is noteworthy that flake NO.21 is not stable, exceptionally. For the flake NO.21, bilayer flake without dopant is more stable than the doped one, because the centre of each carbon ring is a stable position for absorbent. In fact, the boundary H atoms of smaller flake in the both flakes NO. 21 and 22 instead of a parallel position respect to the larger flakes turn toward the larger flake centre. The only difference between these two flakes is that for the flake NO.21, there is one H atom which stops this rotation. While for the flake NO.22, two boundary H atoms stop this rotation toward the larger flake centre. As a consequence, for the flake NO.21, smaller layer optimization position is perpendicular to the graphene flake and two boundary H atoms have been absorbed by two near benzene rings. As a result, two H boundary atoms act similar to two distinctive dopants themselves. Consequently this structure is more stable that doped one in which there is one dopant for the same larger layer.

According to table.2, the arrangement of spin polarization amount according to the flake number is: 25, 18, 17, 26, 19, 23, 14, 16, 20, 24, 15, 22, and 21. In addition, the spin polarization intervals are generally smaller for bilayer GNFs relative to monolayer ones with a similar radius. For instance, for GNFs NO.16 to 26 spin polarization is less than a similar doped monolayer GNF. Furthermore, according to Fig.3, in flake NO.14 with a Li atom between two coupled benzene rings, both surfaces are ferromagnetically spin polarized and strongly correlated (Fig.4). For the flake NO.15, one layer is FM while the smaller layer does not have any spin polarization with 10^{-2} accuracy. Consequently, we have both FM and NM layers in the flake No.15.

For the flake NO.16, like No.14, two surfaces have a common spin density regions (Fig.4). This common joint between two layers happens because of the high concentration of the spin density at the edges. Flake number 17 has two similar flakes doped by one Li in the centre. The important note about this structure is a drastic reduction of the spin density relative to the similar

View Article Online
DOI: 10.1039/C5RA27922D

monolayer flake. However, both layers are still FM. GNF NO.18 is similar to NO.17; a reduction of magnetization in FM layers is noticeable.

In fact for all GNFs, both doped layers are FM, if it be spin polarized. According to table 2 and Fig.3, flake NO.22 is more spin polarized relative to flakes NO.19 to 21, and the same rule applies for the flake NO.24 relative to 23; and the flake NO.26 relative to NO.25. Consequently, the spin polarization is dependent on the second layer size and position. In detail, edge adsorption for the second layer increases FM properties. However, according to Fig. 4 and table.2 for small size flakes, NO.14, 16 and 18, this rule is not correct any more, because the increase of the spin distribution on the edge has entangled two layers.

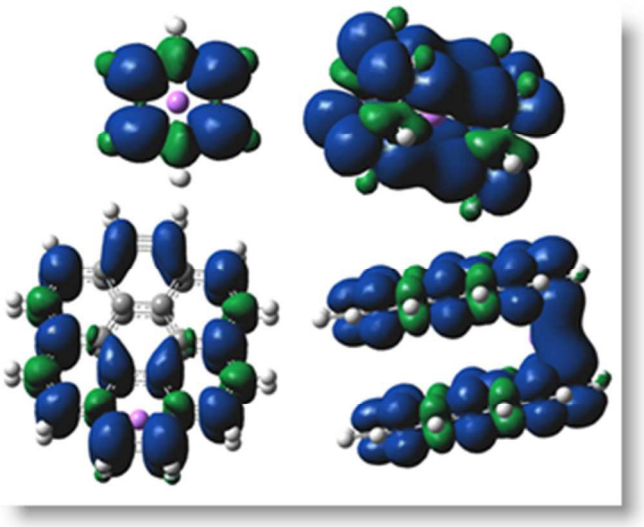

Fig 4.Side view of GNFs NO.14 and 18. As it is visible in the right side of this picture (top and down), the spin density distribution for two different layers have been entangled similar to a joint. The isosurface value is ±0.0004 electrons per cubic atomic unit.

According to table2, there are two effective factors influence bilayer GNFs gap amounts. First, the gap is generally red shifted by increasing the number of C atoms. For instance, between flakes NO.22 and 23, the gap of the second flake is red shifted, because it has more C atoms. The second factor which affects the gap is the second layer position. For instance, between flakes 19 to 22, the later which has benzene layer nearer to the edge has a larger gap, same about flake NO.15 and 16. However, a systematic relation between the Li position and the gap has not been found.

View Article Online
DOI: 10.1039/C5RA27922D

In addition, according to Fig.3, similar to monolayer cases, if a Li atom is adsorbed beside two H atoms or if Li is on a symmetry line passing through such a ring, a tunnel of spin polarized density is visible in the SMM. Indeed, a tunnel of spin polarized regions happens in that vicinity.

Because of a strong concentration of spin up, benzene rings with two H atoms at the edge are the best regions for connection in a circuit.

Application

Suggestions for spin amplifiers

As mentioned earlier, Li-doped single layers are generally better FM in comparison to bilayer graphene. Consequently, doped monolayer structures are better amplifiers. However, in bilayer GNFs, the second layer could be managed for appropriate ferromagnetism and spin polarization. Additionally, between all bilayer flakes, those which have a higher amount of adsorption energy and a large spin polarization are preferable spin amplifiers. Consequently, the author suggests flakes 22 and 24 as spin amplifiers, because these flakes have a high spin density and relative stability. The spin polarization of these bilayer GNFs is also near to the similar monolayer GNFs.

The effect of the temperature on the dopant, at room temperature ($270 < T < 400$ K), is that Li atoms fall in the boundary condition [55]. Moreover, based on previous research [52], the interlayer space are preferable for adsorption. In addition, the current research shows that structures with the benzene or a dopant at the edge are more stable. Consequently, suggested flakes are stable up to room temperature and Li-doped GNFs are SMMs and room temperature spin amplifiers.

A bilayer GNF as an amplifier could act better at higher temperature. In fact, because of the migration of Li and benzene ring to the edge, the spin polarization and the stability of GNFs increase generally. However, the study of managing edge states, of adsorbent type to increase spin density and whether more odd numbers of Li atoms increases spin polarization needs more research.

View Article Online
DOI: 10.1039/C5RA27922D

Spintronic on/off switch based on Li-doped bilayer

Molecular orbitals (MOs) are conduction channels for electrons [56]. These channels can be obstructed (localized) or not (delocalized). Those also can be occupied by electrons or not. Any factor which changes this occupation allows us to tailor the electrical behaviour of the molecule [54]. A non-conducting channel is a localized MO, which cannot connect both ends of the molecule attached to metallic contacts. Furthermore, shapes of frontier molecular orbitals explain qualitatively the conduction of electrons through molecules attached to macroscopic contacts [54]. Based on this analysis, the author suggests a structure similar to Fig.5 for applications in the field of single electron on/off switches. According to Fig.5, Li-doped bilayer GNFs with layers of different sizes could act as a single electron on/off switch. In such a SMM, OMO and UMO concentration switch between layers. Such a switch of molecular orbitals happens because of the repulsive effect of H atoms.

As determined before, the stability and the spin polarization of these structures in comparison with other GNFs are high. In addition, for suggested on/off switch for spintronic purposes, contacts should be added to one layer. Furthermore, based on table2 and Fig.5, it is predictable that this type of switch will have a high on/off ratio, because of the low covering effects of two doped layers with different sizes. However, this ratio will be decreased by the movement of Li atom to the edge of a SMM at higher temperatures (Fig.3).

Memory devices based on Li-doped bilayer

According to Fig.5, when an electron transfers to the LUMO state of the depicted SMMs [56], there is no MO on the larger surface. This define a logical “0” state for a memory device. Moreover, when there is not any electron in the HOMO level, the probability of existence of electron in the smaller layer is zero. This effect define a logical “1” digit. According to Fig.5, for HOMO-2, HOMO-1, HOMO, LUMO, LUMO+1 and LUMO+2 such a switch of states also happens. Consequently, the switch between two layers and this up and down states can be used to define a memory device. Consequently, the author suggests the usage of bilayer graphene SMM as a memory device, as well.

View Article Online
DOI: 10.1039/C5RA27922D

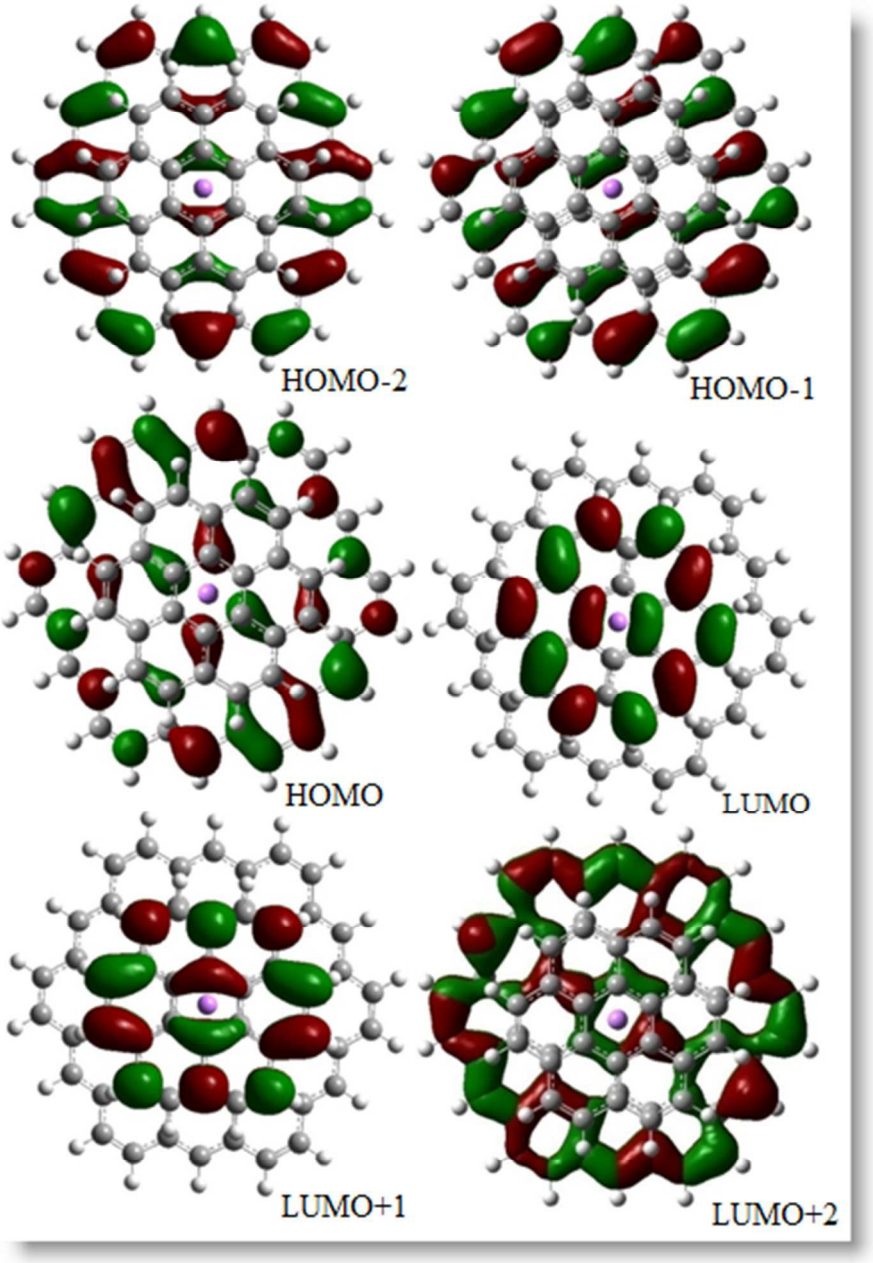

Fig.5. Spin up molecular Orbitals view for bilayer GNF NO.17 which is a doped bilayer graphene with layers of different sizes. According to this figure, for HOMO-2 to LUMO+2, MOs are distributed on one layer. Colour code: red, positive; green, negative. The isovalue is 0.02.

Conclusion

All of the considered doped graphene structures with one Li atom are FM, while a flake doped by two atoms is a NM which does not have any localized spin polarized state. This point makes

View Article Online
DOI: 10.1039/C5RA27922D

it possible to build two FM and NM phases by use of GNFs. Li-doped GNFs are spin polarized and alpha and beta gaps are red shifted by increasing of the size. Furthermore, Li-doped GNFs could be used as spintronic SMMs for room temperature applications, because these flakes generally have more stable edge states. For better conduction of spin polarized current, a contact group should be attached where two H atoms are bonded in a benzene ring. In addition, larger SMMs which have a dopant nearer to the boundary are better FM. In the flakes where dopant is on a ring with two H atoms, spin amplifiers could act better. This point is a positive reason for room temperature applications of doped GNFs as SMMs.

For bilayer graphene, flakes of different sizes have been studied, where the dopant position and the second layer size and place are variable. About the relative stability, flakes with the adsorbent nearer to the edge are more stable. Spin polarization is also dependent on the second layer size and position. Both layers are FM, if it be spin polarized. Additionally, the edge adsorption of the second layer increases FM properties. Furthermore, where two layers are small, because of the high intensity of the spin distribution on the edge, two layers are entangled in each other and spin polarization decreases drastically. Moreover, for bilayer SMMs, the alpha and beta gaps are generally red shifted by the increase of the number of C atoms. In addition, those benzene rings with two H atoms at the edge are the best choices to be used as the contact group in a circuit.

For spintronic purposes, suggested SMMs could be used as spin amplifier, spin on/off switch and memory devices for room temperature applications. Monolayer Li-doped flakes are better FM and also amplifiers. Graphene flakes similar to flakes NO.22 and 24 have high spin density and relative stability; so, those flakes are better spin amplifiers. In addition, bilayer flakes with layers of different sizes could act as an on/off switch and amplifiers, as well. In addition, in these flakes, spin polarized MO switches between layers. According to the switch of MOs, logical “0” and “1” states for molecular memory devices could be achievable.

Acknowledgements

This work was made possible by the facilities of Computational Nanotechnology Supercomputing Centre, Institute for Research in Fundamental Science (IPM). The author is immensely grateful to Dr. Edward McCann for his precious comments on an earlier version of the manuscript.

View Article Online
DOI: 10.1039/C5RA27922D

References

1. Datta, S., *Quantum transport: atom to transistor*2005: Cambridge University Press.
2. Yin, G., et al., *Polarization-induced switching effect in graphene nanoribbon edge-defect junction.* The Journal of chemical physics, 2009. **131**(23): p. 234706.
3. Leuenberger, M.N. and D. Loss, *Quantum computing in molecular magnets.* Nature, 2001. **410**(6830): p. 789-793.
4. Bogani, L. and W. Wernsdorfer, *Molecular spintronics using single-molecule magnets.* Nature materials, 2008. **7**(3): p. 179-186.
5. Wernsdorfer, W., *Molecular Magnets: A long-lasting phase.* Nature materials, 2007. **6**(3): p. 174-176.
6. Christou, G., et al., *Single-molecule magnets.* Mrs Bulletin, 2000. **25**(11): p. 66-71.
7. Gatteschi, D., R. Sessoli, and J. Villain, *Molecular nanomagnets*2006: Oxford University Press.
8. Timm, C. and F. Elste, *Spin amplification, reading, and writing in transport through anisotropic magnetic molecules.* Physical Review B, 2006. **73**(23): p. 235304.
9. Elste, F. and C. Timm, *Transport through anisotropic magnetic molecules with partially ferromagnetic leads: Spin-charge conversion and negative differential conductance.* Physical Review B, 2006. **73**(23): p. 235305.
10. Green, J.E., et al., *A 160-kilobit molecular electronic memory patterned at 1011 bits per square centimetre.* Nature, 2007. **445**(7126): p. 414-417.
11. Drögeler, M., et al., *Nanosecond spin lifetimes in single-and few-layer graphene–hBN heterostructures at room temperature.* Nano Letters, 2014. **14**(11): p. 6050-6055.
12. Drögeler, M., et al., *Nanosecond spin lifetimes in bottom-up fabricated bilayer graphene spin-valves with atomic layer deposited Al_2O_3 spin injection and detection barriers.* arXiv preprint arXiv:1507.02677, 2015.
13. Volmer, F., et al., *Spin and charge transport in graphene-based spin transport devices with Co/MgO spin injection and spin detection electrodes.* arXiv preprint arXiv:1503.01735, 2015.
14. Wang, W.L., S. Meng, and E. Kaxiras, *Graphene nanoflakes with large spin.* Nano Letters, 2008. **8**(1): p. 241-245.
15. Kheirabadi, N., A. Shafiekhani, and M. Fathipour, *Review on graphene spintronic, new land for discovery.* Superlattices and Microstructures, 2014. **74**: p. 123-145.
16. Kim, Y.R., et al., *Electrostatically transparent graphene quantum-dot trap layers for efficient nonvolatile memory.* Applied Physics Letters, 2015. **106**(10): p. 103105.
17. Beljakov, I., et al., *Spin-crossover and massive anisotropy switching of 5d transition metal atoms on graphene nanoflakes.* Nano Letters, 2014. **14**(6): p. 3364-3368.
18. Droth, M. and G. Burkard, *Spintronics with graphene quantum dots.* physica status solidi (RRL)-Rapid Research Letters, 2015. **9999**.
19. Konstantatos, G., et al., *Hybrid graphene-quantum dot phototransistors with ultrahigh gain.* Nat Nano, 2012. **7**(6): p. 363-368.
20. Güttinger, J., et al., *Spin states in graphene quantum dots.* Physical review letters, 2010. **105**(11): p. 116801.
21. Volk, C., et al., *Electronic excited states in bilayer graphene double quantum dots.* Nano Letters, 2011. **11**(9): p. 3581-3586.

View Article Online
DOI: 10.1039/C5RA27922D

22. Potasz, P., et al., *Electronic properties of gated triangular graphene quantum dots: Magnetism, correlations, and geometrical effects.* Physical Review B, 2012. **85**(7): p. 075431.
23. Jacobsen, A., et al., *Transport in a three-terminal graphene quantum dot in the multi-level regime.* New Journal of Physics, 2012. **14**(2): p. 023052.
24. Güttinger, J., et al., *Transport through graphene quantum dots.* Reports on Progress in Physics, 2012. **75**(12): p. 126502.
25. Bischoff, D., et al., *Electronic triple-dot transport through a bilayer graphene island with ultrasmall constrictions.* New Journal of Physics, 2013. **15**(8): p. 083029.
26. Beenakker, C., *Colloquium: Andreev reflection and Klein tunneling in graphene.* Reviews of Modern Physics, 2008. **80**(4): p. 1337.
27. Stampfer, C., et al., *Tunable graphene single electron transistor.* Nano Letters, 2008. **8**(8): p. 2378-2383.
28. Lu, J., et al., *Transforming C60 molecules into graphene quantum dots.* Nat Nano, 2011. **6**(4): p. 247-252.
29. Cancado, L., et al., *Influence of the atomic structure on the Raman spectra of graphite edges.* Physical review letters, 2004. **93**(24): p. 247401.
30. Affoune, A., et al., *Experimental evidence of a single nano-graphene.* Chemical Physics Letters, 2001. **348**(1): p. 17-20.
31. Affoune, A., et al., *Electrophoretic deposition of nanosized diamond particles.* Langmuir, 2001. **17**(2): p. 547-551.
32. Kosynkin, D.V., et al., *Longitudinal unzipping of carbon nanotubes to form graphene nanoribbons.* Nature, 2009. **458**(7240): p. 872-876.
33. Müller, A., et al., *Bilayer graphene quantum dot defined by topgates.* Journal of Applied Physics, 2014. **115**(23): p. 233710.
34. Zhou, Y., et al., *Epitaxial Growth of Asymmetrically-Doped Bilayer Graphene for Photocurrent Generation.* Small, 2014. **10**(11): p. 2245-2250.
35. Fringes, S., et al., *Charge detection in a bilayer graphene quantum dot.* physica status solidi (b), 2011. **248**(11): p. 2684-2687.
36. Schnez, S., et al., *Observation of excited states in a graphene quantum dot.* Applied Physics Letters, 2009. **94**(1): p. 012107.
37. Molitor, F., et al., *Observation of excited states in a graphene double quantum dot.* EPL (Europhysics Letters), 2010. **89**(6): p. 67005.
38. Owens, F.J., *Electronic and magnetic properties of armchair and zigzag graphene nanoribbons.* The Journal of chemical physics, 2008. **128**(19): p. 194701.
39. Huang, B., et al., *Towards graphene nanoribbon-based electronics.* Frontiers of Physics in China, 2009. **4**: p. 269-279.
40. Son, Y.-W., M.L. Cohen, and S.G. Louie, *Energy gaps in graphene nanoribbons.* Physical review letters, 2006. **97**(21): p. 216803.
41. Hod, O., V. Barone, and G.E. Scuseria, *Half-metallic graphene nanodots: A comprehensive first-principles theoretical study.* Physical Review B, 2008. **77**(3): p. 035411.
42. Son, Y.-W., M.L. Cohen, and S.G. Louie, *Half-metallic graphene nanoribbons.* Nature, 2006. **444**(7117): p. 347-349.
43. Wang, W.L., et al., *Topological frustration in graphene nanoflakes: magnetic order and spin logic devices.* Physical review letters, 2009. **102**(15): p. 157201.

View Article Online
DOI: 10.1039/C5RA27922D

44. Pisula, W., X. Feng, and K. Müllen, *Charge-Carrier Transporting Graphene-Type Molecules†.* Chemistry of Materials, 2010. **23**(3): p. 554-567.
45. Emery, N., et al., *Superconductivity of bulk CaC 6.* Physical review letters, 2005. **95**(8): p. 087003.
46. Guzman, D., H. Alyahyaei, and R. Jishi, *Superconductivity in graphene-lithium.* 2D Materials, 2014. **1**(2): p. 021005.
47. Ludbrook, B.L., Giorgio; Nigge, Pascal; Zonno, Marta; Schneider, Michael; Dvorak, David; Veenstra, Christian; Zhdanovich, Sergey; Wong, Douglas; Dosanjh, Pinder; Straßer, Carola; Stohr, Alexander; Forti, Stiven; Ast, Christian; Starke, Ulrich; Damascelli, Andrea,*Evidence for superconductivity in Li-decorated graphene.* 2015arXiv150805925L, 2015.
48. Becke, A.D., *Density-functional thermochemistry. III. The role of exact exchange.* The Journal of chemical physics, 1993. **98**(7): p. 5648-5652.
49. Lee, C., W. Yang, and R.G. Parr, *Development of the Colle-Salvetti correlation-energy formula into a functional of the electron density.* Physical Review B, 1988. **37**(2): p. 785.
50. M. J. Frisch, G.W.T., H. B. Schlegel, G. E. Scuseria, M. A. Robb, J. R. Cheeseman, J. A. Montgomery, Jr., T. Vreven, K. N. Kudin, J. C. Burant, J. M. Millam, S. S. Iyengar, J. Tomasi, V. Barone, B. Mennucci, M. Cossi, G. Scalmani, N. Rega, G. A. Petersson, H. Nakatsuji, M. Hada, M. Ehara, K. Toyota, R. Fukuda, J. Hasegawa, M. Ishida, T. Nakajima, Y. Honda, O. Kitao, H. Nakai, M. Klene, X. Li, J. E. Knox, H. P. Hratchian, J. B. Cross, V. Bakken, C. Adamo, J. Jaramillo, R. Gomperts, R. E. Stratmann, O. Yazyev, A. J. Austin, R. Cammi, C. Pomelli, J. W. Ochterski, P. Y. Ayala, K. Morokuma, G. A. Voth, P. Salvador, J. J. Dannenberg, V. G. Zakrzewski, S. Dapprich, A. D. Daniels, M. C. Strain, O. Farkas, D. K. Malick, A. D. Rabuck, K. Raghavachari, J. B. Foresman, J. V. Ortiz, Q. Cui, A. G. Baboul, S. Clifford, J. Cioslowski, B. B. Stefanov, G. Liu, A. Liashenko, P. Piskorz, I. Komaromi, R. L. Martin, D. J. Fox, T. Keith, M. A. Al-Laham, C. Y. Peng, A. Nanayakkara, M. Challacombe, P. M. W. Gill, B. Johnson, W. Chen, M. W. Wong, C. Gonzalez, and J. A. Pople, *Gaussian 03,* 2004, Gaussian, Inc: Wallingford CT.
51. Kheirabadi, N. and A. Shafiekhani, *The ground state of graphene and graphene disordered by vacancies.* Physica E: Low-dimensional Systems and Nanostructures, 2013. **47**: p. 309-315.
52. Kheirabadi, N. and A. Shafiekhani, *Graphene/Li-ion battery.* Journal of Applied Physics, 2012. **112**(12): p. 124323.
53. Liechtenstein, A.I., et al., *Local spin density functional approach to the theory of exchange interactions in ferromagnetic metals and alloys.* Journal of Magnetism and Magnetic Materials, 1987. **67**(1): p. 65-74.
54. Seminario, J.M., A.G. Zacarias, and P.A. Derosa, *Theoretical analysis of complementary molecular memory devices.* The Journal of Physical Chemistry A, 2001. **105**(5): p. 791-795.
55. Tachikawa, H. and A. Shimizu, *Diffusion dynamics of the li atom on amorphous carbon: a direct molecular orbital-molecular dynamics study.* The Journal of Physical Chemistry B, 2006. **110**(41): p. 20445-20450.
56. Bonaccorso, F., et al., *Graphene photonics and optoelectronics.* Nature photonics, 2010. **4**(9): p. 611-622.

View Article Online
DOI: 10.1039/C5RA27922D

View Article Online
DOI: 10.1039/C5RA27922D

Table of contents

1-Graphic

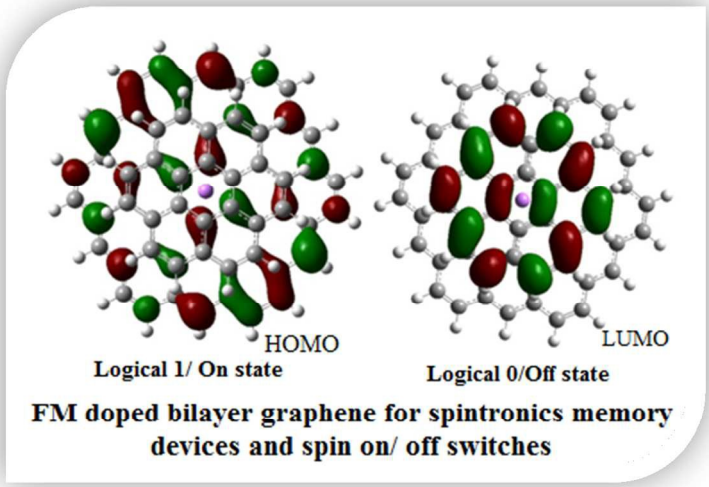

2-one sentence of text

For spintronic purposes, suggested graphene based SMMs could be used as spin amplifier, spin on/off switch and memory devices for room temperature applications.